

Epoxidation of Ethylene with Products of Thermal Gas-Phase Oxidation of *n*-Butane

R. R. Grigoryan^a and S. D. Arsentev^{a, *}

^a*Nalbandyan Institute of Chemical Physics, National Academy of Sciences of the Republic of Armenia, Yerevan, 0014 Armenia*

**e-mail: arsentiev53@mail.ru*

Received July 31, 2019; revised September 29, 2019; accepted October 14, 2019

Abstract—Epoxidation of ethylene with the reactive products formed during thermal gas-phase oxidation of *n*-butane has been carried out under flow conditions with the separation of the zones of generation of radicals and their interaction with ethylene. Butane is oxidized in the first section of a two-section reactor, and ethylene is fed to the second section. It has been found that increasing the residence time of a butane–oxygen mixture in the first section of the reactor from 7 to 13 s increases the ethylene oxide accumulation rate. A further increase in the contact time leads to a decrease in the rate. Similarly, increasing the C₄H₁₀/O₂ ratio in the range of 0.05–0.25 leads to an increase in the rate of accumulation of ethylene oxide. A further increase in this ratio decreases the rate of epoxidation. It has also been found that the temperature dependences of the ethylene oxide accumulation rate in both sections of the reactor pass through a maximum. The obtained data give evidence for the occurrence of the ethylene epoxidation reaction initiated by the *n*-butane oxidation products under the conditions when ethylene itself is slightly oxidized.

Keywords: ethylene, epoxidation, ethylene oxide, butane

DOI: 10.1134/S096554412002005X

Olefin oxides are base petrochemical products with the rapidly growing volume of consumption [1–3]. This is explained by the continuous growth in the industrial production of their derivatives [4, 5]. For example, ethylene glycol, which is the main derivative of ethylene oxide, is used as a reactant in the production of polyethylene terephthalate, a solvent and a plasticizer, as well as in the production of antifreezes and monomers for the fabrication of synthetic fibers [6]. Another derivative, diethylene glycol, is the feedstock in the production of polyester resins and foamed plastics, and dinitroethylene glycol is used as an alternative to nitroglycerin in the production of nonfreezing, impact-resistant dynamite. Nonionic surfactants obtained on the basis of ethylene oxide are very effectively used in oil producing and refining industry [7–9]. Liquid and waxy polymers used as plasticizers and lubricants are obtained via the polymerization of ethylene oxide. Ethylene oxide itself, as well as compounds on its basis, can be used as a fuel [10] and an agent for sterilization of medical devices [11].

In general, industrial-scale production of ethylene oxide can be based on the following three processes: catalytic oxidation of ethylene, noncatalytic oxidation of ethylene, and preparation from ethylene chlorohydrin [12]. To date, only two processes, namely, the oxidation of ethylene over silver catalysts and the alkali treatment on ethylene chlorohydrin, have found industrial application [13]. Of these, the chlorohydrin

method is more efficient. However, the production of ethylene oxide using this process requires the use of chlorine and chlorine-resistant reactor materials and is accompanied by the formation of a significant amount of chlorine-containing wastes polluting the environment.

Catalytic oxidation of ethylene is much more environmentally friendly [14–17]. Currently, almost all ethylene oxide is catalytically obtained on industrial scale. The most effective catalysts for the oxidation of ethylene to its oxide are silver and its compounds [1, 5, 18–20], which make it possible to obtain the target product with the selectivity exceeding 70% [13, 19, 21]. At the same time, the use of silver in catalytic processes is fraught with a number of complex problems. The catalyst fabrication technologies are complex and multistage. In the course of operation, catalysts lose the activity as a result of aging and poisoning [22] and need to be periodically regenerated. The complicating factors are special requirements to the purity of the hydrocarbon feedstock. Sulfur compounds that are natural concomitants of natural hydrocarbon feedstock, arsenic, and acetylene pose the greatest danger for silver catalysts. The presence of other hydrocarbons, hydrogen, and carbon oxides is also undesirable.

Noncatalytic processes for producing ethylene oxide are free from the above disadvantages. As opposed to the catalytic processes, a number of valu-

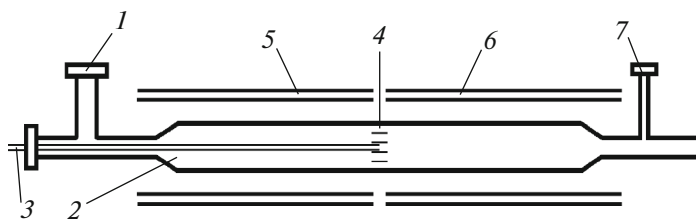
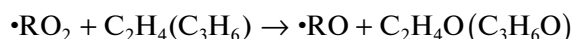


Fig. 1. Scheme of the reactor: (1) connector for feeding the butane–oxygen mixture, (2) first section of the reactor, (3) feeding capillary for ethylene, (4) package of quartz tubes, (5) oven of the first section of the reactor, (6) oven of the second section of the reactor, (7) sampling connector.

able products, such as ethylene oxide, formaldehyde, and organic acids, are formed in the case of homogeneous oxidation of ethylene with oxygen. Currently, ethylene oxide synthesis methods via homogeneous oxidation of ethylene in the gas phase are being developed [23, 24] because this process requires neither an expensive catalyst nor chlorine. In addition, this ethylene oxide production process does not require the gases with purity as high as in the case of the catalytic process. The disadvantage of the process is a wide variety of its products and low selectivity, which is explained by the chain mechanism of occurring transformations and high temperature. However, the development of the theory of chain processes opens new ways for improving gas-phase oxidation reactions of ethylene.

In previous studies [25–29], it was shown that the epoxidation of ethylene and propylene during their thermal gas-phase oxidation involves the interaction of peroxide radicals with the double bond of the olefin according to the reaction



and the rate constants of these reactions were measured. The analysis performed in [30] shows that in the case of thermal gas-phase oxidation of ethylene, this reaction plays the key role and other routes of epoxidation including peroxide epoxidation (which plays the key role in the case of liquid-phase epoxidation of olefins) do not make a substantial contribution to this process. It has also been found that in the process conducted in a two-section reactor, the peroxide radicals generated in the reaction of gas-phase thermal oxidation of methane can effectively epoxidize ethylene [31].

Earlier, epoxidation of ethylene was also studied using co-oxidation of ethylene and butane. It was shown that in this case, the epoxidation of ethylene proceeds at low temperatures, at which ethylene itself is not oxidized [33]. At the same time, the introduction of ethylene into the reaction mixture from the very beginning of the process leads to its untenable consumption for undesired products. Because of this, it was decided to separate the zone of generation of reactive particles formed during the oxidation of the

paraffin hydrocarbon from the epoxidation zone. The choice of the hydrocarbon that generates peroxide radicals has been determined by the fact that alkyl peroxide radicals generated by the oxidation of butane in a two-section reactor accumulate in the second section at concentrations exceeding 10^{-9} mol/cm³ [33, 34].

The aim of this work is to study the process of ethylene epoxidation with reactive compounds generated in the thermal gas-phase oxidation of butane in the case of co-oxidation of ethylene and *n*-butane with the separation of the zones of generation of radicals and their interaction with ethylene.

EXPERIMENTAL

The scheme of the reaction unit for running the ethylene coepoxidation process is presented in Fig. 1. A two-section reactor was used which was a quartz tube of a 20 cm length and a 2 cm diameter. The reactor was divided into separate sections using a partition consisting of a package of quartz tubes. The reactor was heated with two independent electrical ovens, which made it possible to set different temperatures in the reactor sections. A mixture of *n*-butane with oxygen was fed through a seal connector to the first section of the reactor, where the oxidation of butane with the formation of an active medium occurred. Ethylene was fed to the second section of the reactor through a capillary.

The separation and determination of the concentrations of the gaseous products was performed on an LKhM-8MD chromatograph. Methanol, ethanol, acetaldehyde, and ethylene oxide were separated on a column packed with the polymer sorbent Polisorb-1 ($l = 3$ m, $d = 3$ mm, $T_{\text{col}} = 378$ K, $Q = 30$ cm³/min, and helium as the carrier gas). C_1 – C_4 hydrocarbons were separated on a column packed with Silipor-600 ($l = 3$ m, $d = 3$ mm, $T_{\text{col}} = 363$ K, $Q = 24$ cm³/min, and helium as the carrier gas). Hydrogen, oxygen, methane, and CO were separated on a column packed with molecular sieves 5 Å ($l = 2$ m, $d = 3$ mm, $T_{\text{col}} = 363$ K, $Q = 24$ cm³/min, and argon as the carrier gas). In all the cases, a thermal conductivity detector was used.

Table 1. Concentrations of the main products obtained for different contact times in the first and second sections of the reactor. $T_1 = 673$ K, $T_2 = 613$ K, $n\text{-C}_4\text{H}_{10}:\text{O}_2 = 0.117$, and $P = 86.7$ kPa

No.	$Q_1, \text{cm}^3/\text{s}$	$Q_2, \text{cm}^3/\text{s}$	Partial pressure of the reaction products, kPa				
			CH_3OH	CH_3CHO	$\text{C}_2\text{H}_4\text{O}$	HCHO	CO
1	0.51	0.92	0.459	0.526	1.396	0.502	2.14
2	0.63	1.14	0.441	0.542	1.449	0.509	2.13
3	0.76	1.37	0.433	0.561	1.437	0.521	2.12
4	0.83	1.49	0.412	0.583	1.354	0.532	2.03
5	1.03	1.85	0.354	0.592	1.318	0.532	1.95
6	1.28	2.30	0.305	0.588	1.211	0.518	1.63
7	1.34	2.41	0.281	0.467	1.234	0.474	1.23
8	1.45	2.61	0.134	0.372	1.103	0.368	0.91
9	1.52	2.73	0.106	0.296	0.982	0.271	0.45
10	1.59	2.86	0.096	0.254	0.723	0.218	0.23
11	1.92	3.45	0.083	0.186	0.292	0.153	0.09

The flow rates of feeding the mixture to the first and second sections of the reactor (Q_1 and Q_2) were selected in such a way that the concentration of ethylene was the same in all the experiments.

The concentration of formaldehyde was measured using chromotropic acid on a KFK-2 photoelectric colorimeter. For formaldehyde determination, the effluent reaction gases were bubbled through distilled water for a certain time. To increase the contact surface of the gases with the solvent, the bubbler was filled with fine glass cullet. The concentration of formaldehyde in the reactor was calculated by the formula $C = C_b V T_{\text{amb}} / Q t_b T_r$, where C is the concentration in the reactor, mol/cm^3 ; C_b is the concentration in the solution from the bubbler, mol/cm^3 ; V is the volume of water in the bubbler, cm^3 ; Q is the volumetric flow rate of the reactants fed to the reactor, cm^3/s ; t_b is the duration of bubbling, s; and T_{amb} and T_r are the ambient and reactor temperatures, respectively.

If needed, the concentration of formaldehyde was recalculated to the partial pressure according to the formula $P = P_{\text{st}} C N_A T_r / T_{\text{st}} N_L$, where P is the partial pressure, kPa; T_{st} is the standard temperature, 298 K; P_{st} is the standard pressure, 101.308 kPa; N_A is the Avogadro number; and N_L is the Loschmidt number.

RESULTS AND DISCUSSION

The experiments showed that the main products of the process were carbon monoxide, ethylene oxide, acetaldehyde, methanol, and formaldehyde. Ethanol, methane, and carbon dioxide were also detected, but they were in insignificant amounts.

Table 1 presents the concentrations of the main products measured at different flow rates of feeding of the butane–oxygen mixture to the first section of the reactor.

Since the concentration of ethylene oxide at the outlet from the reactor is determined by the difference between its formation and consumption and depends on the concentration gradients of the epoxidizing active particles, we can speak with confidence only about the experimentally measured average rate of ethylene oxide accumulation in the second section of the reactor. This quantity was calculated from the data of Table 1 according to the formula

$$W_{\text{C}_2\text{H}_4\text{O}} = P_{\text{C}_2\text{H}_4\text{O}} / t_2,$$

where $W_{\text{C}_2\text{H}_4\text{O}}$ is the average ethylene oxide accumulation rate, kPa/s; $P_{\text{C}_2\text{H}_4\text{O}}$ is the partial pressure of ethylene oxide at the reactor outlet, kPa; and t_2 is the residence time of the reaction mixture in the second section of the reactor, s. Figure 2 presents the dependence of the average rate of ethylene oxide accumulation on the residence time of the butane–oxygen mixture in the first section of the reactor.

As is seen from Fig. 2, the average rate of accumulation of ethylene oxide is maximum at the residence time of ~ 13 s for the butane–oxygen mixture in the first section of the reactor. In the case of a decrease or increase in the contact time, the rate of accumulation of ethylene oxide sharply decreases. Obviously, its decrease is due to the fact that the oxidation of butane is a degenerate branched process, as a result of which the rate of the process and concentrations of active species depend on the contact time. Since the rate of accumulation of ethylene oxide is associated with the concentration of active particles that come from the first section and the concentration of ethylene was maintained the same in all the experiments (see Table 1), the nonmonotonic dependence of the rate of the process and concentration of the active particles

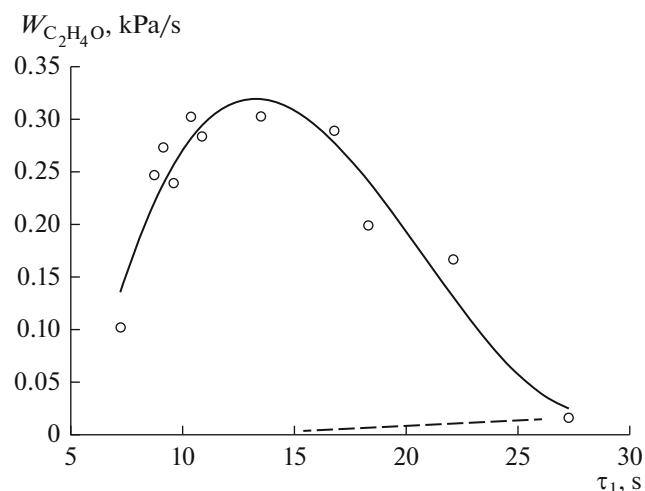


Fig. 2. Dependence of the average rate of accumulation of ethylene oxide on the contact time in the first section of the reactor. $T_1 = 673$ K, $T_2 = 613$ K, $C_4H_{10} : O_2 = 0.117$, and $P = 86.7$ kPa. The dashed line presents the results obtained using argon instead of butane.

arriving from the first section of the reactor on the contact time leads to the appearance of a maximum in the plot of $W_{C_2H_4O}$ versus the residence time of the butane–oxygen mixture (τ_1) in the first section.

For comparison, the dashed line in this same figure presents a similar dependence obtained under the same process conditions but with the replacement of butane by argon in the mixture fed to the first section of the reactor. The experiments showed that the rate of accumulation of ethylene oxide is significantly lower in this case. For example, $W_{C_2H_4O}$ decreases more than 30-fold for $\tau_1 \sim 12$ – 14 s. This result suggests that ethylene is very slowly oxidized under these conditions and the presence of butane sharply increases the generation of particles that epoxidize the olefin.

When the flow rate of the butane–oxygen mixture fed to the first section of the reactor was $Q_1 = 1.92$ cm³/s (Table 1, no. 11), the selectivity of conversion of ethylene to ethylene oxide was $\sim 96\%$. The selectivity was calculated by the formula

$$S = [C_2H_4O] / \Delta[C_2H_4],$$

where S is the selectivity, $[C_2H_4O]$ is the concentration of ethylene oxide at the outlet of the reactor, and $\Delta[C_2H_4]$ is the consumption of ethylene.

According to published data [27], the maximum selectivity for ethylene oxide in the case of ethylene oxidation under standard conditions cannot exceed 67%. Such a limit of selectivity is associated with the fact that some ethylene is consumed for the formation of peroxide radicals. Under the conditions of our experiments in the two-section reactor, the generation of the active particles occurs in the process of oxidation of butane in the first section, while ethylene in the second section is mainly consumed in the epoxidation reaction. As a result, the selectivity of conversion of ethylene to its oxide increases.

Obviously, the rate of oxidation of hydrocarbons and concentrations of radicals during the process depend on the composition of the reaction mixture. In this connection, the influence of the composition of the mixture in the first section of the reactor on the epoxidation process was investigated. Table 2 presents the concentrations of the main products obtained upon varying the butane/oxygen ratio in the mixture fed to the first section of the reactor.

The data of Table 2 were used to plot in Fig. 3 the dependence of the average rate of accumulation of ethylene oxide on the butane/oxygen ratio in the mixture fed to the first section of the reactor.

As is seen from Fig. 3, increasing the n - C_4H_{10}/O_2 ratio in the range from 0.05 to 0.25 leads to a 1.8-fold increase in the average rate of accumulation of eth-

Table 2. Concentrations of the main products obtained for various compositions of the butane–oxygen mixture fed to the first section of the reactor. $T_1 = 673$ K, $T_2 = 613$ K, $Q_1 = 1.30$ cm³/s, $Q_2 = 2.30$ cm³/s, and $P = 86.7$ kPa

No.	$C_4H_{10} : O_2$	Partial pressure of reaction products, kPa				
		CH_3OH	CH_3CHO	C_2H_4O	$HCHO$	CO
1	0.05	0.475	0.227	1.055	0.231	2.10
2	0.07	0.509	0.365	1.907	0.284	1.95
3	0.13	0.563	0.485	1.722	0.424	1.82
4	0.21	0.562	0.531	1.818	0.448	1.79
5	0.25	0.527	0.493	1.901	0.465	1.78
6	0.35	0.512	0.434	1.556	0.432	1.81
7	0.50	0.504	0.421	1.436	0.396	1.81
8	0.79	0.499	0.393	0.870	0.372	1.79
9	0.85	0.483	0.348	0.888	0.353	1.77

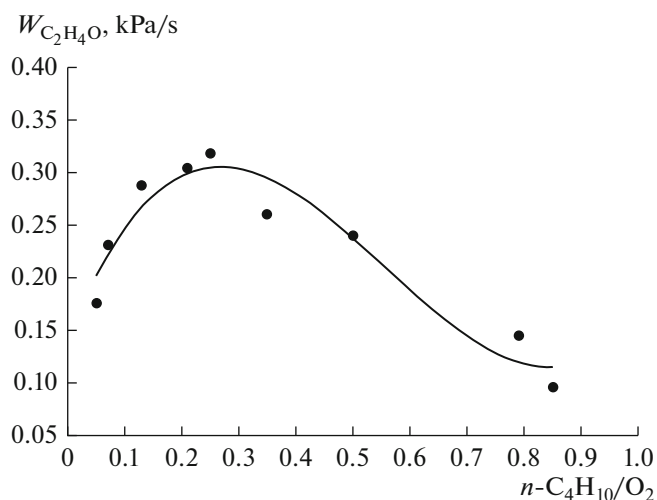


Fig. 3. Dependence of the average rate of accumulation of ethylene oxide on the butane/oxygen ratio in the first section of the reactor. $T_1 = 673$ K, $T_2 = 683$ K, $Q_1 = 1.30$ cm³/s, $Q_2 = 2.30$ cm³/s, and $P = 86.7$ kPa.

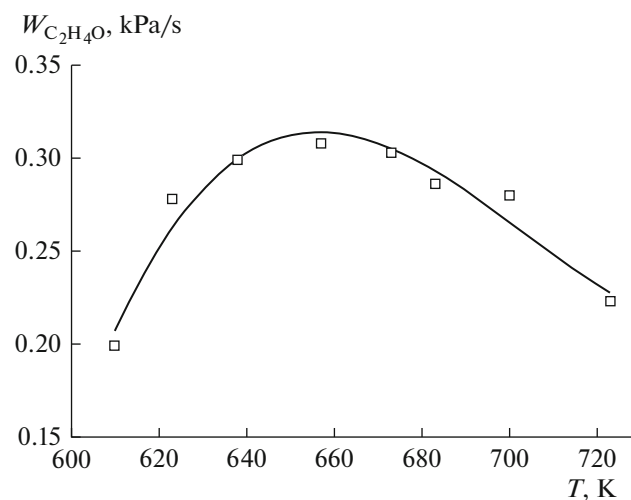


Fig. 4. Dependence of the average rate of accumulation of ethylene oxide on the temperature in the first section of the reactor. $C_4H_{10} : O_2 = 0.21$, $T_2 = 683$ K, $Q_1 = 1.30$ cm³/s, $Q_2 = 2.30$ cm³/s, and $P = 86.7$ kPa.

ylene oxide. A further increase in this ratio leads to a more than twofold decrease in $W_{C_2H_4O}$.

It is known that the intensity of oxidation of hydrocarbons depends on the hydrocarbon/oxygen ratio and passes through a maximum [35, 36]. Obviously, the dependence of the concentration of the active intermediate products promoting the epoxidation of ethylene on the $n-C_4H_{10}/O_2$ ratio also passes through a maximum, thereby explaining the presence of the maximum in Fig. 3.

Since the rate of a chemical process and, hence, the concentrations of active intermediate products (including radicals) depend on temperature, it is obvious that the temperature in the first section of the reactor should affect the rate of formation of ethylene oxide in the second section. The data obtained at dif-

ferent temperatures in the first section of the reactor are presented in Table 3.

Figure 4 shows the dependence of the average rate of accumulation of ethylene oxide on the temperature in the first section of the reactor. The rate of accumulation was calculated based on the data of Table 3.

As is seen from Fig. 4, the average rate of accumulation of ethylene oxide is maximum at the temperature in the first section of $T_1 = 650$ – 660 K. In the case of a decrease or increase in the temperature, the rate of accumulation of ethylene oxide decreases. Obviously, this is associated with the fact that the oxidation of butane is a degenerate branched process, as a result of which the time taken to reach the maximum concentration of active intermediate products, including peroxide radicals, in the first section of the reactor changes with a change in the temperature. At low tem-

Table 3. Influence of the temperature in the first section of the reactor, T_1 , on the yield of the products. $C_4H_{10} : O_2 = 0.21$, $T_2 = 683$ K, $Q_1 = 1.30$ cm³/s, $Q_2 = 2.30$ cm³/s, and $P = 86.7$ kPa

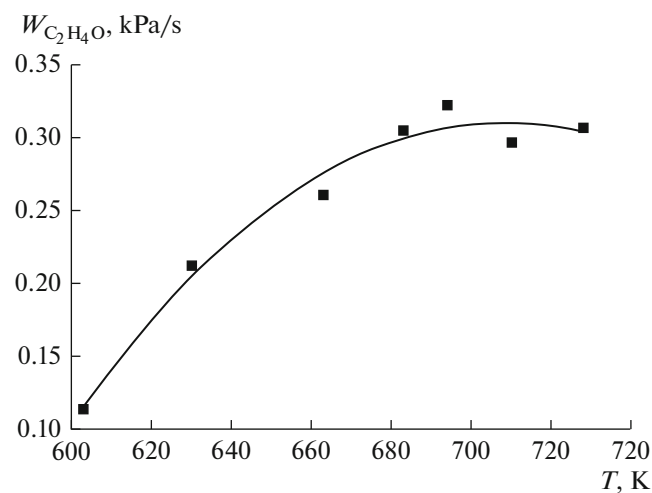
No.	T_1 , K	Partial pressure of reaction products, kPa				
		CH ₃ OH	CH ₃ CHO	C ₂ H ₄ O	HCHO	CO
1	610	0.581	0.549	1.186	0.418	1.72
2	623	0.563	0.544	1.654	0.443	1.75
3	638	0.558	0.536	1.783	0.451	1.78
4	657	0.552	0.533	1.773	0.450	1.78
5	673	0.562	0.531	1.868	0.448	1.83
6	683	0.536	0.512	1.705	0.453	1.91
7	700	0.492	0.486	1.668	0.472	2.16
8	723	0.465	0.434	1.329	0.479	2.31

Table 4. Influence of the temperature in the second section of the reactor, T_2 , on the yield of the products. $C_4H_{10} : O_2 = 0.21$, $T_1 = 673$ K, $Q_1 = 1.30$ cm³/s, $Q_2 = 2.30$ cm³/s, and $P = 86.7$ kPa

No.	T_2 , K	Partial pressure of reaction products, kPa				
		CH ₃ OH	CH ₃ CHO	C ₂ H ₄ O	HCHO	CO
1	603	0.529	0.537	0.770	0.412	1.65
2	630	0.532	0.536	1.370	0.441	1.72
3	663	0.543	0.532	1.602	0.449	1.77
4	683	0.562	0.531	1.818	0.448	1.79
5	694	0.558	0.512	1.887	0.470	1.83
6	710	0.553	0.485	1.702	0.465	1.92
7	728	0.541	0.473	1.720	0.467	2.14

peratures ($T_1 < 640$ K), the concentration of the active particles does not manage to reach the maximum within the set contact time and, because of this, the rate of accumulation of ethylene oxide in the second section is lower than the maximum rate. At temperatures $T_1 > 670$ K, the oxidation process starts decelerating at the set contact time because of the consumption of the reactants, as a result of which the concentration of the active particles entering into the second section decreases. As a result, the rate of ethylene oxide accumulation also starts decreasing, which leads to the appearance of a maximum in the dependence of $W_{C_2H_4O}$ on the temperature in the first section.

Earlier [26], the rate constant of epoxidation of ethylene by alkyl peroxide radicals $\cdot RO_2$ was measured. It was found that the activation energy of this reaction is $E = 57.7$ kJ/mol. Apparently, at such an activation energy, an increase in temperature should increase the rate of epoxidation. In this connection,

**Fig. 5.** Dependence of the average rate of accumulation of ethylene oxide on the temperature in the second section of the reactor. $C_4H_{10} : O_2 = 0.21$, $T_1 = 673$ K, $Q_1 = 1.30$ cm³/s, $Q_2 = 2.30$ cm³/s, and $P = 86.7$ kPa.

experiments at different temperatures were performed in the second section of the reactor, i.e., in the epoxidation zone. The concentrations of the main products experimentally measured upon varying the temperature in the second section of the reactor are presented in Table 4.

The data of Table 4 were used to construct the dependence, shown in Fig. 5, of the average rate of accumulation of ethylene oxide on the temperature in the second section of the reactor.

As is seen from Fig. 5, increasing the temperature in the range of 600–695 K leads to a 2.8-fold increase in the ethylene oxide accumulation rate. Since the conditions of butane oxidation in the first section remain unchanged, i.e., the concentration of the active components coming into the second section of the reactor remains constant, the growth in $W_{C_2H_4O}$ is obviously due to the increase in the rate constant of epoxidation with temperature. In the case of further increase in the temperature, the rate of accumulation of ethylene oxide little changes. Apparently, the increase in the rate constant of epoxidation is compensated by the accelerating consumption of ethylene oxide at high (>700 K) temperatures. This is also evidenced by the decrease in the concentrations of other oxygen-containing products (Table 4) and the increase in the concentration of the deep oxidation product, carbon monoxide. At the temperature in the second section of $T_2 = 683$ K, the selectivity of ethylene conversion to ethylene oxide is $S \sim 87\%$ at the degree of ethylene conversion of $\sim 6\%$.

CONCLUSIONS

The character of the dependence of the rate of ethylene oxide accumulation on the butane/oxygen ratio in the first section of the reactor and temperature in both sections gives evidence for the initiation of the ethylene epoxidation process by the products of *n*-butane oxidation under the conditions when ethylene itself is very slowly oxidized.

FUNDING

The Nalbandyan Institute of Chemical Physics, National Academy of Sciences of the Republic of Armenia is funded by the Government of the Republic of Armenia.

CONFLICT OF INTEREST

The authors declare no conflict of interest to be disclosed in this paper.

REFERENCES

1. *The Global Ethylene Oxide Market 2019* (Williams & Marshall Strategy, 2019). www.researchandmarkets.com/reports/4665297/the-global-ethylene-oxide-market#rela3-3150666.
2. *Propylene Oxide: Chemical Economics Handbook* (IHS Markit, 2019). <https://ihsmarkit.com/products/propylene-oxide-chemical-economics-handbook.html>.
3. S. Rebsdats and D. Mayer, Ethylene Oxide, in *Ullman's Encyclopedia of Industrial Chemistry*, 7th Ed. (Wiley-VCH, Weinheim, 2012), vol. 13, p. 548.
4. *Mono-Ethylene Glycol (MEG): Production, Market, Price and Its Properties* (Plastics Insight, 2016). www.plasticsinsight.com/resin-intelligence/resin-prices/mono-ethylene-glycol-meg.
5. *Ethylene Glycols: Chemical Economics Handbook* (IHS Markit, 2018). <https://ihsmarkit.com/products/ethylene-glycols-chemical-economics-handbook.html>.
6. H. Yue, Y. Zhao, X. Ma, and J. Gong, *Chem. Soc. Rev.* **41**, 4218. 2012.
7. *Surfactants: Fundamentals and Applications in the Petroleum Industry*, Ed. by L. L. Schramm (Cambridge Univ. Press, Cambridge, 2000).
8. N. V. Sautina, Candidate's Dissertation in Chemistry (Kazan, 2009).
9. B. R. Fakhruddinov, Candidate's Dissertation in Chemistry (Kazan, 2001).
10. I. Glassman and R. A. Yetter, *Combustion*, 4th Ed. (Elsevier, Amsterdam, 2008).
11. H. Shintani, *Biocontrol Sci.* **22**, 1 (2017).
12. W. A. Smit, A. F. Bochkov, and R. Caple, *Organic Synthesis: The Science behind the Art* (The Royal Society of Chemistry, Cambridge, 1998).
13. M. G. Slin'ko, *Vestn. Ross. Akad. Nauk* **71**, 635 (2001).
14. S. Pak, A. Rokitski, and S. Kavabata, RU Patent No. 2495715; *Byull. Izobret.*, No. 29 (2013).
15. D. M. Rekers and A. A. Smaardijk, RU Patent No. 2462461; *Byull. Izobret.*, No. 27 (2012).
16. N. Rizkalla, R. Klein, and S. B. Milne, US Patent No. 5945551 (1999).
17. E. M. G. A. van Kruchten, D. M. Rekers, and M. J. P. Slapak, RU Patent No. 2466123; *Byull. Izobret.*, No. 31 (2012).
18. A. S. Yusuff, A. A. Adeyi, and O. O. Jeffrey, *Int. J. Sci. Eng. Res.* **6**, 1626 (2015).
19. J. R. Lockemeyer, D. Reinalda, and R. C. Yeates, RU Patent No. 2314156; *Byull. Izobret.*, No. 1 (2008).
20. *Kirk-Othmer Encyclopedia of Chemical Technology*, 4th Ed. (Wiley, New York, 1994), p. 1112.
21. M. Ya. Rubank and Ya. B. Gorokhovatskii, *Incomplete Catalytic Oxidation of Olefins* (Tekhnika, Kiev, 1964) [in Russian].
22. G. L. Montrasi, G. R. Tauszik, M. Solari, and G. Leonfanti, *Appl. Catal.* **5**, 359 (1983).
23. D. Kh. Safin, G. P. Ashikhmin, Kh. V. Mustafin, and A. I. Chebareva, *Khim. Prom-st' Segodnya*, No. 4, 25 (2003).
24. D. Kh. Safin and A. A. Petukhov, *Khim. Prom-st' Segodnya*, No. 8, 45 (2005).
25. S. D. Arsentev and A. A. Mantashyan, *Catal. Lett.* **13**, 125 (1980).
26. A. A. Mantashyan, S. D. Arsentev, L. A. Khachatryan, and O. M. Niazyan, *Combust. Flame* **43**, 221 (1981).
27. A. A. Mantashyan and S. D. Arsent'ev, *Kinet. Katal.* **22**, 1389 (1981).
28. A. A. Mantashyan, S. D. Arsentev, and R. R. Grigoryan, *React Kinet. Catal. Lett.* **21**, 347 (1982).
29. A. A. Mantashyan, S. D. Arsent'ev, and R. R. Grigoryan, *Kinet. Katal.* **27**, 782 (1986).
30. S. D. Arsent'ev, Doctoral Dissertation in Chemistry (Yerevan, 1996) [in Russian].
31. R. R. Grigoryan, S. D. Arsentev, and A. A. Mantashyan, *Pet. Chem.* **51**, 448 (2011).
32. S. D. Arsent'ev and A. A. Mantashyan, *Arm. Khim. Zh.* **33**, 778 (1980).
33. T. R. Simonyan and A. A. Mantashyan, *Arm. Khim. Zh.* **32**, 691 (1979).
34. T. R. Simonyan and A. A. Mantashyan, *Arm. Khim. Zh.* **32**, 757 (1979).
35. *Technological Combustion*, Ed. by S. M. Aldoshin and M. I. Alymov (RAN, Moscow, 2018), ch. 5, p. 114 [in Russian].
36. V. Arutyunov, N. Pogosyan, M. Pogosyan, et al., *Chem. Eng. J.* **329**, 231 (2017).

Translated by E. Boltukhina